

Entropy in Toy Regge models

M.A. Braun

Dept. of High Energy physics, Saint-Petersburg State University,
198504 S.Petersburg, Russia

September 4, 2024

Abstract

The probabilistic interpretation of the standard Regge-Gribov model with triple pomeron interactions is discussed. It is stated that introduction of probabilities within this model is not unique and depends on what is meant under the relevant substructures. The traditional interpretation in terms of partons (quarks and gluons) is shown to be external to the model, imported from the QCD, and actually referring to the single pomeron exchange without interactions. So this interpretation actually forgets the model as such. Alternative probabilities based on the pomerons as basic quantities within the model are discussed. Two different approaches are considered, based either on the pomerons in Fock's expansion of the wave function or on pomeron propagators in Feynman diagrams. These pomeron probabilities and entropy turn out to be very different from the mentioned standard ones in the purely probabilistic treatment. The entropy, in particular, either rises with the rapidity and saturates at a certain fixed value or first rises, reaches some maximum and goes down to zero afterwards. Possible observable manifestations of these probabilities and entropy are to be seen in the distributions of the cross-section in powers n assuming that their dependence of the coupling constants g to the participants is presented as a series in g^n .

1 Introduction

In the studies of the high-energy behavior of the amplitudes generated by strong interactions a notable place has been taken by the Regge-Gribov models based on the exchange of local pomerons evolving in rapidity and self-interacting with a non-Hermithean Hamiltonian. Being essentially a semi-phenomenological approach, such models describe well the bulk features of high-energy interactions with certain well-defined phenomenological parameters, such as the intercept and slope of the pomeron and strength of its imaginary self-coupling. Defined initially in the two-dimensional transverse world they unfortunately cannot be solved exactly beyond the quasi-classical approximation or in the renormalization group approximation in the vicinity of perturbatively found fixed points. For this reason much attention was given in the past to the approximation of zero slope "Toy models", in which the models reduce to fields depending only on rapidity ("zero-dimensional" in the transverse variables). In this approximation the models actually transform to one dimensional quantum mechanical systems living in the imaginary time $t = -iy$, where y is the rapidity, and a peculiar non-hermithean Hamiltonian symmetric in p and q .

Some years ago it was proposed to look at toy Regge-Gribov models (TRGM) in the framework of the so-called statistical reaction-diffusion approach [1]. In this approach the system

was described by a set of probabilities P_n for the creation and decay of a given number n of quasi-particles (e.g. pomerons). In fact much earlier this probabilistic approach was developed in the context of dipole scattering in the QCD as a toy model for dipole-dipole scattering in the approximation of the so called "big loops", which describes fan diagrams attached to the projectile and inverse fan diagrams attached to the target joined at some middle rapidity y_0 between the rapidities y and zero of the projectile and target [2]. It was formulated exclusively in terms of probabilities $P_n(y)$ with a particular evolution equation in y . The total probability P_n was presented as a convolution of probabilities for the joining fan contributions, schematically

$$P = P(y_0) \otimes P(y - y_0). \quad (1)$$

On physical grounds (projectile-target symmetry) one would prefer $y_0 = y/2$ and with this choice (1) was used in several applications [2, 3]. However in fact (1) does depend on y_0 except in the limit $y \rightarrow \infty$ when it corresponds to the unitarity in the t -channel in the BFKL framework. Since then much effort has been directed to achieve independence of this transitional rapidity y_0 , which concentrated on the change of the probabilities P_n within this approach [2, 4, 5, 6, 7, 8]. Note that in the Regge-Gribov field theoretical approach this independence (or "t-channel unitarity") is automatic, since it simply corresponds to the trivial relation

$$e^{-Hy} = e^{-Hy_0} e^{-H(y-y_0)}$$

where H is the Hamiltonian. So attempts to restore y_0 independence at finite y in the probabilistic approach inevitably lead to field models with Hamiltonians much more complicated than in TRGM, with inclusion of infinite number of different multipomeron vertices. In this paper we restrict ourselves to the standard TRGM with only triple pomeron vertices and so leave more sophisticated models outside our attention.

Returning to TRGM, in [1] it was noted that the standard one with only a triple pomeron interaction does not admit a simple probabilistic interpretation since the probabilities P_n introduced in the analogy with the statistical approach do not preserve positivity with the growth of rapidity. However in [3] it was noted that if only splitting (or merging) vertices are retained in the Hamiltonian, when the amplitude reduces to the fan diagram approximation, after some manipulations one returns to the above discussed probabilistic models with well-defined probabilities P_n .

In this note we try to reconsider the probabilistic interpretation of the standard TRGM. We note that the definition of probabilities P_n in the model is far from being unique and depends on what is taken to be the basic substructures. In the standard probabilistic approach they are partons borrowed from the QCD (quarks and gluons). So the corresponding probabilities and entropy can be called partonic. However staying strictly within TRGM we do not see any partons. Rather the relevant basic quantities are pomerons characterized by Fock's representation of the wave function $\Psi(y)$

$$\Psi(y) = \sum_n c_n(y) \Psi_n. \quad (2)$$

where Ψ_n are states with n pomerons. Unlike the standard Quantum Mechanics $\Psi(y)$ has a norm which is not definite positive. Obviously coefficients c_n in some way characterize the relative contribution of n pomerons at rapidity y . Based on these considerations one can try to introduce probabilities P_n to find n pomerons in the system. These pomeronic probabilities will be different from the partonic ones introduced in the probabilistic approach.

In TRGM one can pass to real wave functions and Hamiltonian. In the simplified quasi-classical approximation, when the amplitude can be found analytically, one finds that $c_n(y)$ can be both positive and negative and $|c_n(y)|$ can be greater than unity (and in fact grow

indefinitely as $y \rightarrow \infty$). So it is impossible to directly relate c_n to some probabilities. However there is a simple (but certainly not unique) way out. Having in mind that $|c_n(y)|$ grow with n and y one can define the probabilities as

$$P_n(y) = \frac{|c_n(y)|}{R^n(y)}, \quad R(y) > 0 \quad (3)$$

and search for $R(y)$ from the requirement

$$Z(y) = \sum_{n=1} P_n(y) = 1 \quad (4)$$

With so found $R(y)$ probabilities P_n satisfy all requirements for probabilities

$$P_n(y) \geq 0, \quad \sum_n P_n(y) = 1$$

and correctly describe the relative contribution of a given number n of pomerons. So they can be safely taken as the desired pomeronic probabilities. The weak point of this definition is the possibility to solve (4) for a positive $R(y)$. However as we shall see this obstacle does not arise.

We shall see in Section 3.2 that for the case when there occurs only splitting (or merging) of pomerons these probabilities are quite different from those which figure in the common probabilistic models. They have a completely different behavior at large y and a different entropy.

The described method is not the only one which can be used to introduce the probability to have n pomerons. In fact this depends on what one defines as an n -pomeron state. Some alternative (although with a limited application) will be discussed in Section 3.3. It will lead to still more different behavior of the probabilities and entropy.

2 Standard TRGM

In this section we recall the well-known facts about the zero-dimensional ("Toy") standard Regge-Gribov model. The "state" in the model is characterized by the wave function $\Psi(y)$ depending on rapidity y and evolving in y according to the quasi-Schroedinger equation

$$\frac{d\Psi(y)}{dy} = -H\Psi(y) \quad (5)$$

where H is the non-Hermithean Hamiltonian depending on the operators $\psi(y)$ and $\psi^\dagger(y)$ for annihilation and creation of pomerons. After transformation to new operators

$$\phi^\dagger = -iu, \quad \phi = -iv$$

the Hamiltonian becomes real

$$H = -\mu uv + \lambda uv(u + v). \quad (6)$$

The operators u and v are subject to the abnormal commutation relation

$$[v, u] = -1. \quad (7)$$

The vacuum state satisfies $v\Psi_0 = 0$. All other states are obtained by application of u on the vacuum. In particular

$$\Psi_n = u^n \Psi_0$$

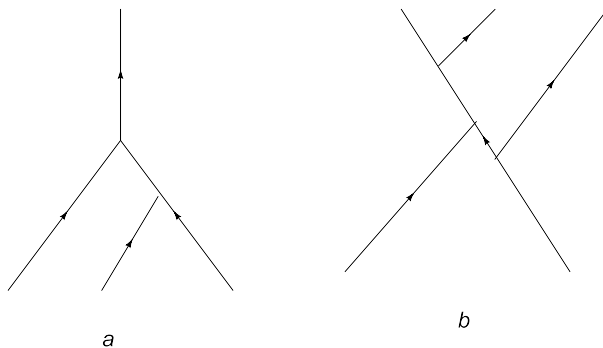


Figure 1: Tree diagrams for proton-nucleus (a) and nucleus-nucleus (b) scattering

is a state with n pomerons. In the u -representation, when u is the operator of multiplication,

$$v = -\frac{\partial}{\partial u}$$

so that the Schroedinger equation (5) becomes an equation in partial derivatives in y and u .

This equation can be technically solved either by expanding in the eigenstates $\Psi^{(n)}$ of the Hamiltonian or by direct evolution by, say, the Runge-Kutta method, as in [3]. In the free theory ($\lambda = 0$) the energy spectrum is evidently $E_n = -\mu_n$, $n = 0, 1, 2, \dots$, so that with $\mu > 0$ (supercritical pomeron) all non-trivial solutions grow indefinitely as $y \rightarrow \infty$. However, as was shown long ago, the interaction radically changes this behavior showing the decisive influence of quantum corrections (loops). As was established in [9] at small λ/μ the ground state takes a small positive value

$$E_0 = \frac{\mu\rho}{\sqrt{2\pi}}e^{-\rho^2/2}, \quad \rho = \frac{\mu}{\lambda} \quad (8)$$

and the wave function slowly goes to zero at $y \rightarrow \infty$.

In the direct evolution one uses the differential equation (in the u -representation)

$$\frac{\partial\Psi(y, u)}{\partial y} = -\left(\mu u \frac{\partial}{\partial u} - \lambda u^2 \frac{\partial}{\partial u} + \lambda u \frac{\partial^2}{(\partial u)^2}\right)\Psi(y, u) \quad (9)$$

with the initial condition, taken typically in the eikonal approximation

$$\Psi(0, u) = 1 - e^{-g_1 u} \quad (10)$$

where g_1 is the pomeron-nucleon coupling in the projectile. The scattering AA amplitude is then given as [3]

$$\text{Im } \mathcal{A}(y) = \Psi(y, g_2) \quad (11)$$

where g_2 is the pomeron-nucleon coupling in the target at rapidity y .

This well-known information by itself however tells us nothing about the statistical characteristics of the model.

3 The quasi-classical approximation. Fan diagrams

In the quasi-classical approximation the scattering amplitude reduces to a set of tree diagrams shown in Fig. 1 *a* for hA scattering and Fig. 1 *b* for AA scattering. In this approximation the

standard TRGM was studied by D.Amati *et al.* long ago [10]. They searched for the solution of the equations of motion

$$\begin{aligned} \dot{u} &= \frac{\partial u}{\partial y} = \frac{\partial H}{\partial v} = -\mu u + \lambda(2uv + u^2), \\ \dot{v} &= \frac{\partial v}{\partial y} = -\frac{\partial H}{\partial u} = \mu v - \lambda(2uv + v^2). \end{aligned} \quad (12)$$

under boundary conditions

$$u(Y) = g_2, \quad v(0) = g_1 \quad (13)$$

where Y is the rapidity of the target with the projectile at rest and g_2 and g_1 are the couplings to external sources. The physical quantity of interest was action \mathcal{A}

$$\mathcal{A} = \lambda \int_0^Y dy v^2 u + g_1 u(0), \quad (14)$$

which determined the scattering matrix. However they were not able to find the solution explicitly at all rapidities but only in the limit $Y \gg 1$.

3.1 Reaction-diffusion probabilities

An especially simple case occurs when field u couples only once to the projectile (nucleon). Then one can drop the term with the product uv in the first equation (12) and obtain the evolution equation for u only. The corresponding amplitude is then given by a set of fan diagrams propagating from the projectile (nucleon) to the target (nucleus). Fig. 1 *a.* and can be found explicitly [11]. The wave function $\Psi(y, u)$ in the u representation is then [3]

$$\Psi(y, u) = \frac{g_1 u e^{\mu y}}{1 + \frac{\lambda u}{\mu} (e^{\mu y} - 1)}. \quad (15)$$

Having this simple and explicitly known solution one may try to interpret the amplitude in terms of probabilities. In [1] the fan case was interpreted as a particular case of a reaction-diffusion process. Following this approach the probabilities to have n partons were introduced in [3] as follows. Following (2) present $\Psi(y, u)$ as a power series in u

$$\Psi(y, u) = \sum_{n=1} c_n(y) u^n. \quad (16)$$

The evolution equation for Ψ generates a system of equations for coefficients $c_n(y)$:

$$\frac{dc_n(y)}{dy} = \mu n c_n(y) - \lambda(n-1)c_{n-1}(y), \quad c_{-1}(y) = 0. \quad (17)$$

Rescale $y = \bar{y}/\mu$ and present

$$c_n(\bar{y}) = \frac{1}{n!} \left(-\frac{\mu}{\lambda} \right)^{1-n} \nu_n(\bar{y}) \quad (18)$$

to obtain an equation for ν_n

$$\frac{d\nu_n(\bar{y})}{d\bar{y}} = n\nu_n(\bar{y}) + n(n-1)\nu_{n-1}(\bar{y}). \quad (19)$$

Note that this equation does not depend on μ nor on λ . Now introduce probability P_n by the relation

$$\nu_n(\bar{y}) = \sum_{k=n}^{\infty} P_k(\bar{y}) \frac{k!}{(k-n)!} \quad (20)$$

with the inverse relation

$$P_n(\bar{y}) = \sum_{k=n}^{\infty} (-1)^{k-n} \frac{\nu_k(\bar{y})}{n!(k-n)!}. \quad (21)$$

One finds that P_n satisfy the evolution equation in \bar{y}

$$\dot{P}_n(\bar{y}) = -nP_n(\bar{y}) + (n-1)P_{n-1}(\bar{y}). \quad (22)$$

With $P_n(0) = \delta_{n1}$ the solution is

$$P_n(y) = e^{-\mu y} a^{n-1}, \quad a = 1 - e^{-\mu y} \quad (23)$$

and the property

$$\sum_{n=1} P_n(y) = 1 \quad \text{at all rapidities.} \quad (24)$$

So taking into account that P_n are positive one can assume that P_n give some probabilities. Precisely the same probabilities were introduced in previous papers in the probabilistic approach (see e.g. [12]). Considering the model as a simplified QCD the probabilities have been interpreted as the ones to have n partons (quarks and gluons) in the system. At $y \gg 1$ one finds $a \simeq 1$ and the probabilities do not depend on n . This fact was interpreted in [12] as a manifestation of achieving the maximally entangled state and "information scrambling" in terms of the information theory.

The entropy following from the probabilities (23) is

$$S(y) = \mu y - e^{\mu y} a \ln a. \quad (25)$$

At large y this entropy grows linearly $S(y) \sim \mu y$. It is shown in Fig. 2 by the upper curve. From (22) it follows that the average \bar{n} satisfies a simple equation

$$\frac{d\bar{n}(y)}{dy} = \mu \bar{n}, \quad \bar{n}(y) = \sum_{n=1} n P_n(y) \quad (26)$$

with the general solution

$$\bar{n}(y) = C e^{\mu y}. \quad (27)$$

Note that neither P_n nor \bar{n} depend on the pomeron coupling λ in TRGM. With $P_n(0) = \delta_{n1}$ one has $\bar{n}(y) = e^{-\mu y}$. In the spirit of the parton-hadron duality the emitted partons have been related to emitted hadrons, so that the probabilities and entropy have been related to observed hadron multiplicities. In this way the entropy (25) has been treated as an observable quantity to be found from the experimental data [13, 14].

Staying within TRGM these results are easily interpreted. Due to the AGK cancelations [15] in the quasi-classical approximation inclusive cross-section coming from all nontrivial diagrams, like shown in Fig 1, cancel and all contribution comes exclusively from the zero-order diagram, that is, the single pomeron exchange, as $C e^{-\mu y}$ where C depends on the sort of the emitted particle. Of course it does not depend on λ being the zero order term in the perturbative expansion. This agrees with the average \bar{n} interpreted as the average number of emitted hadrons in the probabilistic approach. TRGM by itself does not know about the inner structure of the

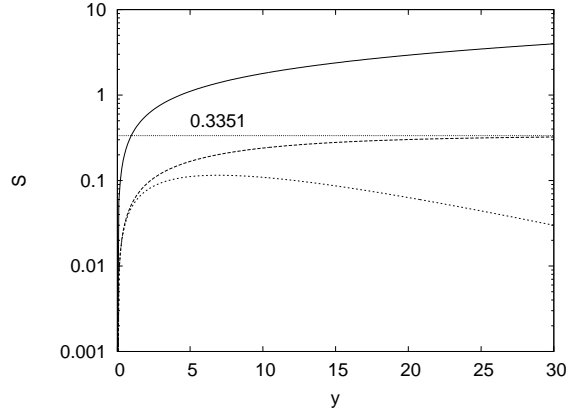


Figure 2: Entropy for the fan amplitude with $\mu = 0.1$ and $\lambda = 0.01$ as a function of rapidity. The upper curve shows entropy (25) from the reaction-diffusion approach. The middle curve shows entropy (36) from the rescaling approach. The lower curve shows entropy (52) from the diagrammatic approach

pomeron exchange, so the probabilities P_n are external to the model supplemented to it by the relation to the QCD. The transformations (18) to (22) proposed in [1, 3] serve to artificially relate c_n and P_n and in this way they liquidate TGRM almost completely leaving only the zero order term. the single pomeron exchange. The net effect of these transformations seems to impose the AGK cancelations on the model.

It is important to note that these partonic P_n do not refer directly to the number of pomerons in the Fock expansion of the wave function (16). Therefore one can alternatively study probabilities of a different sort, describing the structure of the system not in terms of partons absent in the system and artificially brought by analogy with the QCD but rather in terms of pomerons, which are in fact actual components of the system. Possibilities to introduce such pomeronic probabilities and entropy will be considered in the next chapters.

3.2 Number of pomerons from $c_n(y)$. Rescaling method.

. As stated in the Introduction ne can define the number of pomerons n directly from the expansion (16) as the power of u . adequately rescaling coefficients $c_n(y)$ and defining the probabilities as

$$P_n(y) = |c_n(y)|R^{-n}(y), \quad (28)$$

where $R(y)$ is found as a positive solution of the equation

$$Z(R) = \sum_{n=1} \frac{|c_n|}{R^n} = 1. \quad (29)$$

Actually this procedure is to rescale positive $|c_n(y)|$ by factor P^n to obtain probabilities with the necessary properties

Let us see what this rescaling method gives for fan diagrams. From (15) putting $g_1 = 1$ we find

$$|c_n| = \frac{\rho}{a} \left(\frac{a}{\rho(1-a)} \right)^n, \quad \rho = \frac{\mu}{\lambda}. \quad (30)$$

Correspondingly the probabilities are

$$P_n = \frac{\rho}{a} \left(\frac{a}{\rho R(1-a)} \right)^n \quad (31)$$

with the norm

$$Z(R) = \frac{\rho}{a} \sum_{n=1} \left(\frac{a}{\rho R(1-a)} \right)^n = \frac{1}{R(1-a) - a/\rho}. \quad (32)$$

Condition $Z(R) = 1$ determines the contribution from a single pomeron exchange

$$R = \frac{a + \rho}{\rho(1-a)}. \quad (33)$$

With this R the probabilities determined from (28) are found to be

$$P_n = \frac{\rho}{a} \left(\frac{a}{a + \rho} \right)^n. \quad (34)$$

At $y = 0$ we have $a \rightarrow 0$ and $P_n(y = 0) = \delta_{n1}$ as expected. At $y > 0$ the probabilities are falling with n as powers

$$P_{n+1} = P_n \frac{a}{a + \rho}.$$

In the high-energy limit ($a \rightarrow 1$) we obtain $P_n \sim (1 + \rho)^{-n}$. The average number of pomerons is

$$\bar{n} = \sum_{n=1} n P_n = \frac{\rho + a}{\rho}. \quad (35)$$

and the corresponding entropy is given by

$$S = -\frac{\rho}{a} \sum_{n=1} \left(z^n \ln \frac{\rho}{a} + n z^n \ln z \right), \quad z = \frac{a}{a + \rho},$$

and after some calculations

$$S = \frac{a + \rho}{\rho} \ln(a + \rho) - \frac{a}{\rho} \ln a - \ln \rho = \bar{n} \ln \bar{n} - (\bar{n} - 1) \ln(\bar{n} - 1). \quad (36)$$

At $y = 0$ we get $\bar{n} = 1$ and $S = 0$. With the growing y both the average number of pomerons and entropy $S(y)$ grow monotonously until finite limits:

$$\bar{n}_\infty = 1 + \frac{1}{\rho}, \quad S_\infty = \frac{1 + \rho}{\rho} \ln(1 + \rho) - \ln \rho. \quad (37)$$

For the free theory $\rho \rightarrow \infty$ we correctly get $P_n = \delta_{n1}$ and $S = 0$. This entropy is shown in Fig. 2 by the middle curve. The horizontal line marks its limit $S_\infty = 0.3551$.

One may ask if these pomeron probabilities and entropy are observable. The answer is yes. According to (11) the scattering amplitude is obtained after substitution $u \rightarrow g_2$ in $\Psi(y, u)$ where g_2 is the coupling to the nucleon in the target. So distribution in n means the distribution in powers n of the dependence of the amplitude on g_2 . So one can observe n by studying the scattering on the target with different values of g_2 , which corresponds to different spatial interaction points governed by the transverse distribution $T_A(b)$ in the nucleus target.

This definition of probabilities has the advantage of being directly based on the number n of pomerons in the development (16) of the wave function in the fan diagram approximation. However in the quasi-classical approximation it is technically very difficult to introduce it for more complicated diagrams like Fig. 1 *b*, when the solution cannot be obtained in the form (16) but only from the quasi-classical equations of motion. A new definition of pomeron probabilities valid for any diagrams in the quasi-classical approximation will be presented in the next chapter.

3.3 Number of pomerons from the diagrams

To define the number of pomerons one may forget about the expansion (16) and consider instead the amplitude as a set of Feynman diagrams. One may define the number of pomerons n as the number of pomeron propagators in the diagram. It may correspond to the bare pomeron, that is simply the line, or the 'physical' or 'full' pomeron, that is the full two-reggeon Green function consisting of the bare line with all loop insertions. The problem with the second choice is that it is very difficult to locate physical pomerons in the general way. To do that one has to consider skeleton diagrams made of full pomerons, each of them containing an infinite number of bare pomerons. We do not know any technique which allows to find the number of full pomerons in a diagram in any general way. But this problem disappears once we restrict ourselves to the quasi-classical approximation neglecting the loops. Then the physical pomeron becomes identical with the bare one and the number of pomerons is just the total number of lines. Of course this definition of the number of pomerons is quite different from their definitions n in the expansion of the wave function (16). But it has a clear physical meaning and, which is important in the quasi-classical picture, can be applied to the tree-diagrams of any structure, including both Fig. 1 *a* and *b*.

Let a Feynman diagram contain E external lines I internal lines and V vertices. With the triple interaction relevant for Regge models one has the relation $2I + E = 3V$. The number of loops L in a connected diagram is $L = I - V + 1$. In the quasi-classical approximation we take the number n of pomerons as

$$n = E + I \quad (38)$$

with $L = 0$. Then the number of pomerons can be uniquely expressed via E or via V

$$n = E + V - 1 = 2E - 3 = 2V + 1. \quad (39)$$

Note that n is odd, so that with this choice probabilities to find an even number of pomerons are zero $P_{2N} = 0$, $N = 0, 1, 2, \dots$

In the quasi-classical approximation only tree diagrams survive shown in Fig. 1 *a* for hA scattering and Fig. 1 *b* for AA scattering. If the couplings to the projectile and target are g_1 and g_2 respectively, then the contribution with $E = N_1 + N_2$ external lines will be proportional to $g_1^{N_1} g_2^{N_2}$. To simplify we consider a simple case $g_1 = g_2 = g$ (identical nuclei). Then the contribution from n pomerons will be proportional to g^n where $n = 2N - 3$. The pomerons with this new definition are different from those in Fock's expansion (16) used in the previous approach. They are counted in a different manner. Say for the diagram in Fig 1 *a* the number of external lines is $N = 4$ and so the number of pomerons determined from the diagram is $n = 5$, although the latter comes from the term u^3 in (16) and the number of pomerons in the previous definition is only 3.

To pass to probabilities we present \mathcal{A} as a series in powers of g

$$\mathcal{A} = \sum_{N=2} (-1)^N g^N A_N, \quad N = 1, 2, \dots, \quad n = 2N - 3. \quad (40)$$

So the number of pomerons is always odd and we take into account that the sign of contributions is alternating with N . We are going to present A_N as a product of the probability P_n to have n pomerons multiplied by the contribution to A from these n pomerons R^n , that is, as

$$A_N = R^n P_n, \quad n = 2N - 3 \quad (41)$$

where P_n are positive and properly normalized

$$\sum_{N=2} P_n = 1, \quad n = 2N - 3. \quad (42)$$

Using the scaling procedure from the previous section we construct

$$X_N(R) = \frac{A_N}{R^n}, \quad n = 2N - 3$$

and the norm $Z(R)$ depending on R

$$Z(R) = \sum_{N=2} X_N(R), \quad n = 2N - 3. \quad (43)$$

obeying $Z(R) = 1$. Then we take

$$P_n = X_N(R) = \frac{A_N}{R^n}, \quad n = 2N - 3 \quad (44)$$

and have

$$A_N = R^n \frac{A_N}{R^n} = P_n R^n, \quad n = 2N - 3$$

as desired with the properly normalized P_n .

Let us see how this technique works for fan diagrams. In this case taking the coupling to both proton and nucleus equal to g we have the amplitude

$$\mathcal{A} = \frac{g^2 e^{\mu y}}{1 + \frac{g}{\rho}(e^{\mu y} - 1)} = \frac{g^2}{1 - a - ga/\rho} \quad (45)$$

where $\rho = \mu/\lambda$ and a was defined in (23). Developing in powers of g we get in (40)

$$A_N = (1 - a)^{-N+1} \left(\frac{a}{\rho}\right)^{N-2}. \quad (46)$$

So in our technique

$$X_N = (1 - a)^{-N+1} \left(\frac{a}{\rho}\right)^{N-2} R^{-2N+3} \quad (47)$$

and

$$Z(R) = \frac{1}{R(1 - a) - a/(\rho R)}$$

where we use

$$\sum_{N=2} x^N = \frac{x^2}{1 - x}, \quad \sum_{N=2} N x^N = (2 - x) \frac{x^2}{(1 - x)^2}. \quad (48)$$

The equation for R is obtained as

$$R^2(1 - a) - R - \frac{a}{\rho} = 0$$

with a positive solution

$$R = \frac{1 + \sqrt{1 + 4a(1 - a)/\rho}}{2(1 - a)}. \quad (49)$$

The probabilities turn out to be

$$P_n = \frac{\rho R(\rho R + a)}{a^2} \left(\frac{a}{\rho R + a}\right)^N, \quad n = 2N - 3 \quad (50)$$

The average number of pomerons \bar{n} is given by

$$\bar{n} = 2\bar{N} - 3, \quad \bar{N} = \frac{2\rho R + a}{\rho R} \quad (51)$$

and the entropy is

$$S = \ln \frac{\rho R + a}{\rho R} + \frac{a}{\rho R} \ln \frac{\rho R + a}{a}, \quad (52)$$

where we once more used (48).

The found probabilities and entropy are radically different from what was obtained previously. They depend on λ via ρ and as $\lambda \rightarrow 0$ they correctly go to δ_{n1} . They strongly diminish with the number of pomerons. Indeed we have

$$P_{n+2} = P_n \frac{a}{\rho R + a}, \quad n = 1, 3, 5, \dots \quad \text{with} \quad P_1 = \frac{\rho R}{\rho R + a} \quad (53)$$

where the pomeron contribution is

$$R = ce^{\mu y}, \quad c = \frac{1}{2} \left(1 + \sqrt{1 + 4a(1-a)/\rho} \right), \quad 1 < c < \frac{1}{2} (1 + \sqrt{1 + 1/\rho}). \quad (54)$$

When rapidity grows also R grows and the fall of P_n becomes more and more pronounced. At very high y the probabilities return to their values at $y = 0$. Correspondingly the entropy S starts at $S = 0$ then grows achieving its maximum at approximately $\mu y = 0.7$ for $\rho = 1$ and slowly falls to zero afterwards, as illustrated in Fig. 2 for $\mu = 0.1$ and $\lambda = 0.01$ by the lowest curve.

4 Quasi-classical approximation. Multiple fans

Staying within the approximation with only splitting of pomerons one can find explicit amplitudes for the case when the projectile interacts more than one time with the pomeron. In the eikonal approximation this corresponds to taking expression (10) for the initial amplitude. Simple derivation then gives the wave function at any rapidity [3]

$$\Psi(y, u) = 1 - \exp \left[- \frac{g_1 u e^{\mu y}}{1 + \frac{u}{\rho} (e^{\mu y} - 1)} \right]. \quad (55)$$

We recall that $\rho = \mu/\lambda$ and g_1 is the coupling of the pomeron to the projectile (nucleon). Using this expression one can find coefficients $c_n(y)$ in the expansion (16) and from them introduce the probabilities, either following the reaction-diffusion approach passing as before

$$c_n(y) \rightarrow \nu_n(y) \rightarrow P_n(y)$$

or by our rescaling method via

$$P_n(y) = |c_n(y)|/R(y), \quad \sum_{n=1} P_n(y) = 1.$$

However explicit construction of $c_n(y)$ from (55) is quite cumbersome and we prefer to act in a different way. We shall calculate either c_n or probabilities themselves at $y = 0$ and then evolve them to higher rapidities using the evolution equations.

4.1 Reaction-diffusion probabilities

To find the probabilities one commonly introduces a generating function

$$\Phi(y, u) = \sum_{n=1} P_n(y) u^n \quad (56)$$

subject to the obvious conditions

$$\Phi(y, 0) = 0, \quad \Phi(y, 1) = 1 \quad (57)$$

following from its structure and normalization of P_n . It has long been known that due to evolution equations (22) function $\Phi(y, u)$ obeys the equation

$$\frac{\partial \Phi(\bar{y}, u)}{\partial \bar{y}} = (u^2 - u) \frac{\partial \Phi(\bar{y}, u)}{\partial u}, \quad \bar{y} = \mu y. \quad (58)$$

Its solution satisfying the boundary conditions (57) is [3]

$$\Phi(\bar{y}, u) = \frac{1}{b} \left(e^{-\bar{\rho}(1-u)/(1-au)} - e^{-\bar{\rho}} \right) \quad (59)$$

where $\bar{y} = \mu y$, $a = 1 - \exp(-\bar{y})$, $\bar{\rho} = g_1 \rho$ and $b = 1 - \exp(-\bar{\rho})$.

For the eikonal wave function no term constant in u is present, so that in (16) and (18) $c_0(y) = \nu_0(y) = 0$ due to (17). At $u = 0$ we get from (20)

$$P_0(y) + \Phi(y, 1) = P_0(y) + 1 = 0,$$

which determines the nonphysical provability $P_0(y)$ to be equal to minus unity..

At $y = 0$ we have $a = 0$ and

$$\Phi(0, y) = \frac{1}{b} \left(e^{\bar{\rho}(1-u)} - e^{-\bar{\rho}} \right) \quad (60)$$

From this expression by multiple differentiation we find the probabilities at $y = 0$

$$P_n(0) = \frac{e^{-\bar{\rho}}}{b} \frac{\bar{\rho}^n}{n!}, \quad n \geq 1. \quad (61)$$

The average n at $y = 0$ is found to be $\bar{n}(0) = \bar{\rho}/b$.. From (27) it follows then that at all rapidities

$$\bar{n}(y) = \frac{\bar{\rho}}{b} e^{\mu y}. \quad (62)$$

This corresponds to multiple pomeron exchanges in eikonal diagrams.

Probabilities (61) in turn determine coefficients $\nu_n(0)$ by (20). For $n \geq 1$

$$\nu_n(0) = \sum_{k=n} P_k(0) \frac{k!}{(k-n)!} = \frac{e^{-\bar{\rho}}}{b} \sum_{k=n} \frac{\bar{\rho}^k}{(k-n)!} = \frac{1}{b} \bar{\rho}^n$$

and coefficients $c_n(0)$ via $\nu_n(0)$ are found to be

$$c_n(0) = -(-1)^n \frac{1}{n!} \bar{\rho}^{1-n} \frac{1}{b} \bar{\rho}^n = -(-1)^n \frac{1}{n!} \frac{\bar{\rho}}{b}.$$

The obtained $c_n(0)$ correspond to the eikonal wave function with a specific normalization

$$\Psi(0, u) = \frac{\bar{\rho}}{b} \left(1 - e^{-g_1 u} \right). \quad \bar{\rho} = g_1 \rho. \quad (63)$$

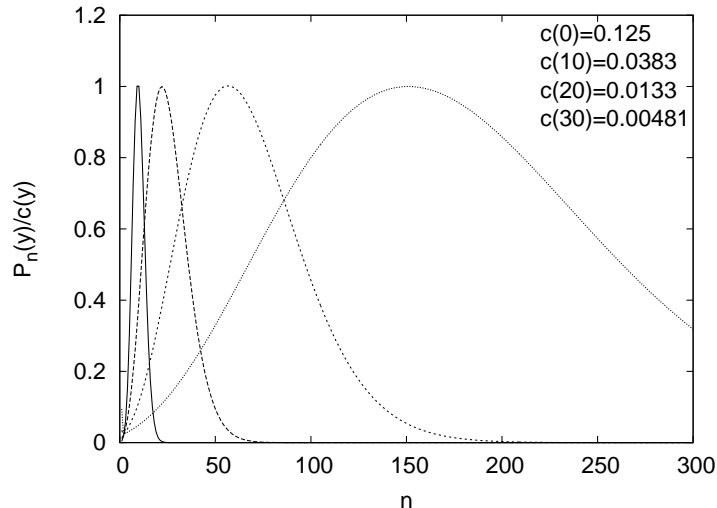


Figure 3: Probabilities to have n pomerons for eikonal fans in the reaction-diffusion approach for $0 \leq n \leq 300$. Shown are rescaled probabilities $P_n(y)/c(y)$ to achieve equal maxima of the curves, which correspond to $y = 0, 10, 20, 30$ from left to right. Values of $c(y)$ are correspondingly 0.125, 0.0383, 0.0133 and 0.00491.

As $g_1 \rightarrow 0$ the normalization coefficient tends to unity and we get

$$\Psi(0, u)_{g_1 \rightarrow 0} = g_1 u, \quad (64)$$

that is the initial state for a single fan. In this limit we find from (61) $P_1 = 1$ and all P_n for $n > 1$ equal to zero as expected.

With many fans $\bar{\rho}$ is different from zero and from (61) one sees that the probabilities are distributed among many partons. As a result the entropy becomes greater than zero already at $y = 0$ although the initial state corresponds to a given wave function. This occurs because we fix the microstates as corresponding to a given number of partons, so that the initial state is rather an ensemble of states with a different number of partons.

The probabilities at $y > 0$ can be obtained from (61) using evolution equations (22). We cutoff the number of partons n at $n = N = 300$. Below we present our numerical results for our typical case $\mu = 0.1$ and $\lambda = 0.01$. We take $g_1 = 1$ so that $\bar{\rho} = \rho = 10$. In Fig. 3 we show the probabilities $P_n(y)$ for $y = 0, 10, 20, 30$ ($\bar{y} = 0, 1, 2, 3$). For illustrative purposes we rescale the probabilities to have equal maxima (around unity). One sees that the spread in the number n of pomerons grows with rapidity covering nearly all values $n < 300$ at $y = 30$. In Fig. 4 we show the entropy for $0 < y < 30$. As stressed at $y = 0$ the entropy is greater than zero

$$S(0) = 2.561.$$

With the growth of y the entropy grows practically linearly similar to the single fan case. The abrupt bending of the curve at $y > 27$ does not reflect the actual behavior but only the result of a breakdown of evolution due to accumulation of errors within the adopted precision.

4.2 The rescaling approach

Contrary to the reaction-diffusion approach, which needs a particular normalization of the initial wave function, the rescaling method can work with the original eikonal wave function

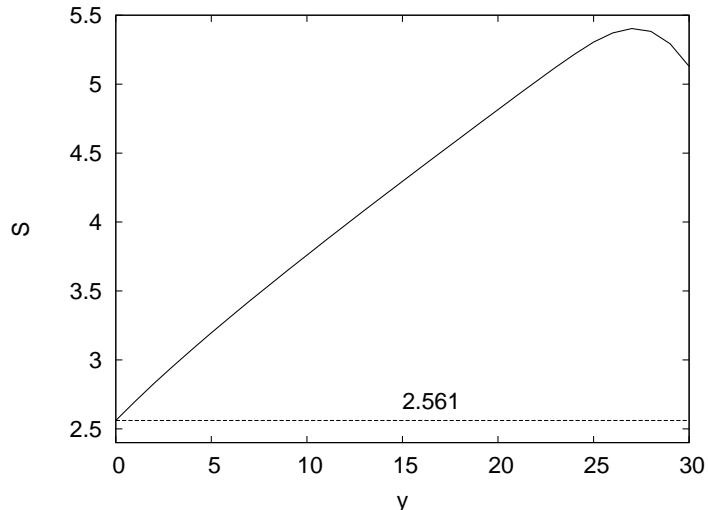


Figure 4: Entropy $S(y)$ for eikonal fans in the reaction-diffusion approach. Bending of the curve at $y > 27$ is only due to the evolution breakdown.

for which at $y = 0$ the coefficients in the expansion in powers u^n are $c_n(0) = -(-1)^n g_1^n / n!$. As before we put $g_1 = 1$. Starting from $c_n(0)$ we use Eqs. (17) and evolve $c_n(y)$ to higher rapidities. Then, as described, we define P_n according to Eqs. (28) and (42).

In our numerical calculations we took $\mu = 0.1$ and $\lambda = 0.01$ as before. Eqs (17) were cutoff at $n = N = 80$. Our results for the entropy are shown in Fig. 5. in the left panel (the upper curve) and in the right panel (practically a constant). As before the entropy is greater than zero already at $y = 0$

$$S(0) = 0.8121.$$

5 Quasi-classical approximation. AA scattering

Now we proceed to the general case of AA scattering illustrated in Fig. 1b. Unlike the fan case the action in the general can only be found by numerical methods. One may consider two different techniques to this aim. The older method proposed in [10] used evolution in rapidity of one of the fields (say u) down from y where it is equal to g_2 according to the first Eq, (12) in which v is expressed via u and the total energy E , which does not change during evolution. Afterwards one has to determine E from the condition $v(0) = g_1$. This method proved to be convenient for analytic approach employed in [10] but turns out to be cumbersome and restricted to rather low values of the coupling constant.

A much more efficient method was used in our (also rather old) iterative method in which one solved the equations of motion (12) using the mixed field from previous iterations. In more detail, one starts evolving u from its value g_2 at y down to zero taking $v = 0$ in the mixed term and v from its value g_1 at rapidity zero up to y taking $u = 0$ in the mixed term. This gives our initial solution u_0 and v_0 . Then iterations are repeated taking the admixed field from the previous iteration, that is, according to

$$\begin{aligned} \dot{v}^{(n+1)} &= \mu v^{(n+1)} - \lambda v^{(n+1)^2} - 2v^{(n+1)}u^{(n)}, \\ \dot{u}^{(n+1)} &= -\mu u^{(n+1)} + \lambda u^{(n+1)^2} + 2\lambda u^{(n+1)}v^{(n)}. \end{aligned}$$

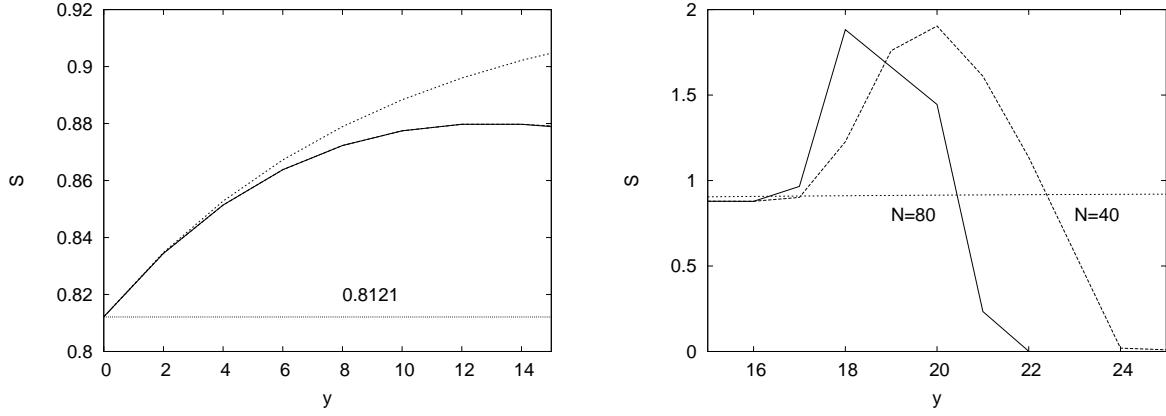


Figure 5: Entropy for AA scattering from the rescaling method with cutoff $n < N$ in the evolution equation for P_n for the multiple fans and full quantum model. The results for the multiple fans are shown in the left panel by the upper curve and in the right panel by practically the constant curve, The results for the full quantum case for $y = 20$ are practically independent of N are shown in the left panel by the lower curve. The results for $y > 20$ for $N = 40, 80$ and 160 are shown in the right panel.

Iterations are stopped when the resulting u and v stop changing.

In fact in our method to find the entropy we need to know terms in the action of a given power of the coupling constant $g = g_1 = g_2$. To do this we develop u and v in powers of g , the dependence on them following from the initial conditions:

$$u = \sum_{N=1} g^N b_N, \quad v = \sum_{N=1} g^N a_n \quad (65)$$

(with $a_0 = b_0 = 0$). The evolution equations transform into the system of evolution equations for a and b :

$$\dot{a}_N = \mu a_N - \lambda \sum_{M=0}^N a_M a_{N-M} - 2\lambda \sum_{M=0}^N a_M b_{N-M}, \quad (66)$$

$$\dot{b}_N = -\mu b_N + \lambda \sum_{M=0}^N b_M b_{N-M} + 2\lambda \sum_{M=0}^N b_M a_{N-M}. \quad (67)$$

These equations are to be solved at each step of our iterational procedure. At the first step one takes $b_n = 0$ in (66) and $a_n = 0$ in (67). At the following steps one takes b_n in (66) and a_n in (67) from the previous iteration.

Numerical results

We applied the iterative procedure to find the action for $\mu = 0.1$ and $\lambda = 0.01$, which are the popular values extracted from the comparison with the data. Taking the symmetric case with $g_1 = g_2 = 1$ we obtained the following values for action \mathcal{A} at $y = 10 \div 50$

$$\mathcal{A}(y) = 2.052, 3.569, 5.406, 7.400, 9.413, \quad \text{at } y = 10, 20, 30, 40, 50. \quad (68)$$

We do not present more detailed values for the action. since we are actually not interested in them as a whole. To determine the probabilities P_n to find n pomerons we split the total action in parts proportional to g^N where $g = g_1 = g_2$ is the common coupling constant to both nuclei

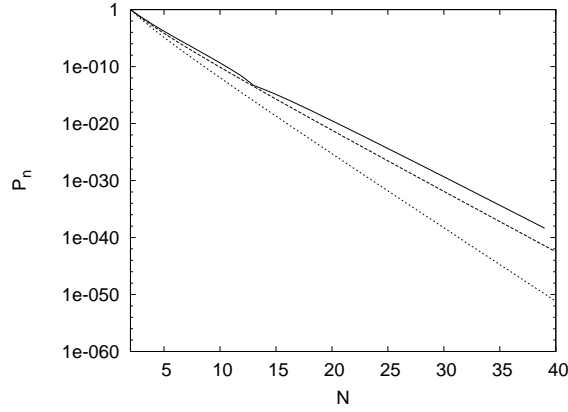


Figure 6: Probabilities P_n to find $n = 2N - 3$ pomerons as a function of N for the general quasi-classical case with $\mu = 0.1$ and $\lambda = 0.01$. The curves from up to bottom correspond to $y = 7.5, 15$ and 22.5

to get

$$\mathcal{A} = \sum_{N=2} \mathcal{A}_N g^N, \quad \mathcal{A}_N = \lambda \int_0^Y dy \sum_{M=0}^N b_M(y) \sum_{L=0}^{N-M} a_L(y) a_{N-M-L}(y) + b_{N-1}(0) \quad (69)$$

where a_N and b_N are the coefficients in (65) obeying Eqs. (66)) and (67).

The system of equations (66) and (67) was solved iteratively for $N = 1, 2, \dots, N_{max}$ as described above. We chose $N_{max} = 40$. Recalling that the number of pomerons is $n = 2N - 3$ this allows to find the probabilities for the maximal number $n_{max} = 77$ pomerons.

As expected the solution of (66) and (67) gave \mathcal{A}_N violently oscillating with N with the amplitude growing fast with rapidity and achieving values of the order 10^{70} for $N = 40$ and $Y = 40$. Summation over $N \leq N_{max}$ gives absurd values for action, which is to be expected, since action is not at all analytic in g . However the results allow to employ our procedure to extract the probabilities described in Section 3. The values of the pomeron exchange found in this way grow with y as $e^{\mu y}$ and the probabilities P_n go down with n very fast. In Fig. 6 we show these probabilities at three typical rapidities 7.5, 15 and 22.5. The logarithmic scale illustrates the fast diminishing of the probabilities with N .

The resulting entropy is shown in Fig. 7 for $y = 0 \div 40$. The AA entropy is found to be significantly higher than for fans, but the overall trend with rapidity is the same. It rises achieving its maximal value at $Y \sim 7$ and then slowly falls at higher Y going to zero at $Y \gg 1$ and so demonstrating vanishing entanglement at high rapidities.

6 Full quantum model

6.1 Reaction-diffusion approach

In [1] an attempt was made to introduce the probability to create pomerons in the same way as for the fan diagram approximation. Namely starting from the same expansion (16) they got a system of evolution equation for c_n generalizing (17)

$$\frac{dc_n(y)}{dy} = \mu n c_n(y) - \lambda(n-1)c_{n-1}(y) + \lambda n(n+1)c_{n+1}. \quad (70)$$

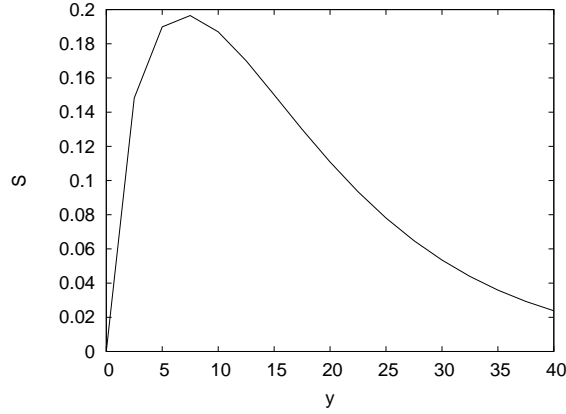


Figure 7: Entropy for the general quasi-classical amplitude with $\mu = 0.1$ and $\lambda = 0.01$ as a function of rapidity

Introducing then ν_n and P_n by the same Eqs. (18) and (20) they obtained a system of equations for P_n , which generalized Eq. (22)

$$\dot{P}_n(\bar{y}) = -nP_n(\bar{y}) + (n-1)\rho_{n-1}(\bar{y}) + \lambda(n+1)(n+2)\rho_{n+2}(\bar{y}) - \lambda n(n+1)\rho_{n+1}(\bar{y}), \quad n = 0, 1, 2, \dots \quad (71)$$

They tried to interpret P_n satisfying this equation as the probabilities to find n partons in the quantum case. However they commented that this immediately met with the difficulty to guarantee positiveness of P_n necessary for such interpretation although they assured that this was irrelevant for their particular purpose in [1].

To see the problem and estimate its scope we evolved $P_n(y)$ according to Eq. (71) for $\mu = 0.1$ and $\lambda = 0.01$ up to $y = 30$ starting from $P_n(0) = \delta_{n1}$, which corresponds to pA scattering (now with loops). Our results depend on the cutoff $n < N$ in Eq. (71).

Generally at all y with the growth of n P_n first diminish smoothly until a certain n when they start oscillating around zero. With the growth of y these oscillations start earlier and their amplitude grows, so that the interpretation of P_n becomes impossible. This is illustrated in Fig. 8 with $n \leq N = 80$. Oscillations begin at $n = 77$ when $y = 9$, at $n = 45$ when $y = 18$ and already at $n = 9$ when $y = 27$ with the amplitude of subsequent oscillations growing with n and y . At $n = 80$ this amplitude grows from 10^{-18} to 100 and 10^{30} at $y = 9, 18$ and 30 respectively. If one takes greater cutoff $N = 160$ then at $y = 9$ the probabilities do not change until $n = 80$. Afterwards they continue to smoothly diminish staying above unity until $n = 160$ when they start oscillations with the amplitude of order 10^{-34} . At higher y the situation worsens. At $y = 18$ oscillations start already at $n = 15$ with the amplitude around unity and at still higher y the probabilities loose any sense with oscillations at all n with ever growing amplitudes reaching order 10^{130} . As a conclusion, one can interpret P_n as a probability only at low rapidities $y < 10 \div 15$. At higher rapidities this interpretation is possible up to certain $n = 1, 2, \dots, n_{max}$ determined by staying inside interval $[0, 1]$.

Accordingly we tentatively calculated the entropy summing over only the states n for which $0 \leq P_n \leq 1$. The results are shown in Fig. 9 for different cutoffs $N = 40, 80$ and 160. As one observes a reasonable entropy is found only at $y \leq 17$, when it turns out to be independent of the cutoff. At higher y the entropy strongly depends on the cutoff and is not trustworthy.

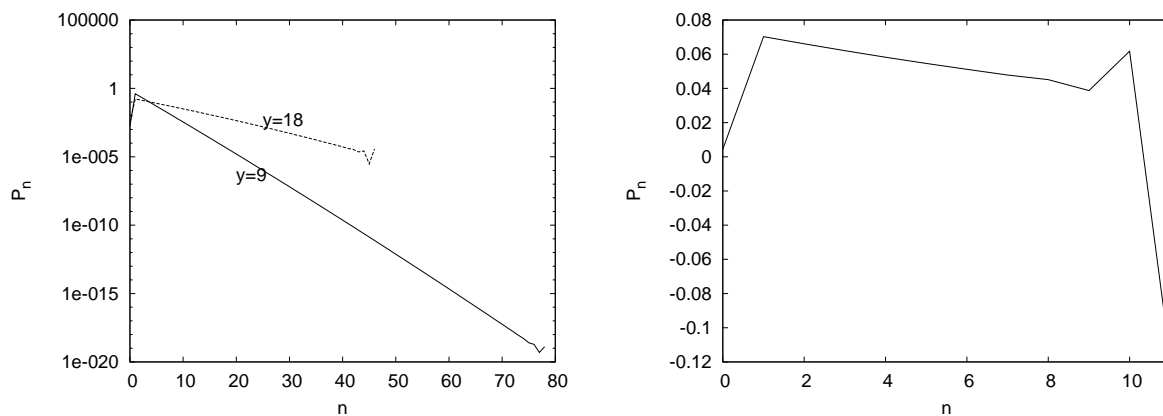


Figure 8: Probabilities P_n from the reaction-diffusion approach with cut $n < 80$ in the evolution equation for P_n . at $y = 9$ and 18 (left panel) and $y = 27$ (right panel)

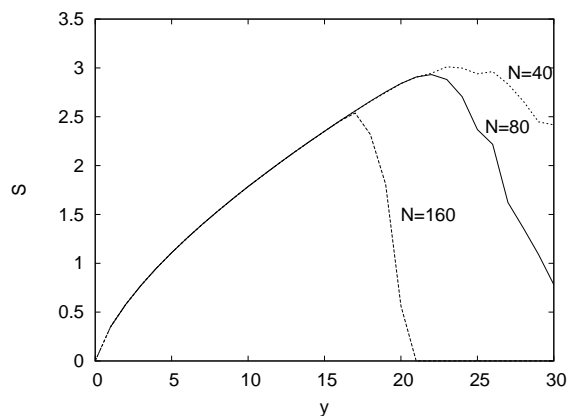


Figure 9: Entropy from the reaction-diffusion approach with cuts $n < N$ in the evolution equation for P_n . Summation over n restricted to its values for which $0 \leq P_n \leq 1$

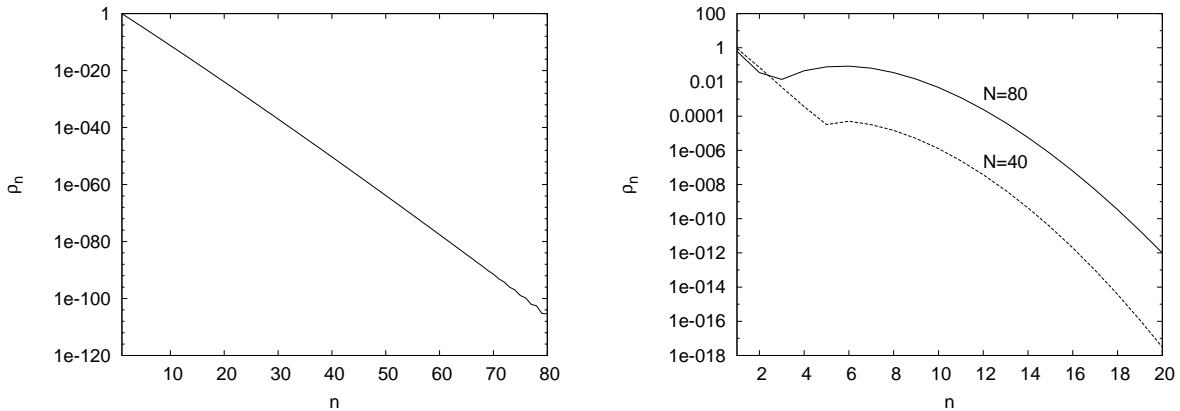


Figure 10: Probabilities P_n for pA scattering from the rescaling method with cutoff $n < N$ in the evolution equation for P_n . at $y = 10$ (left panel) and $y = 27$ (right panel)

6.2 Rescaling method

Unlike the reaction-diffusion approach our rescaling method introduced for the quasi-classical case in Section 4.2 is perfectly applicable also for the quantum case. One solves the system of equations (70) for $c_n(y)$ and introduces the probabilities P_n according to (28) and (42):

pA scattering

For pA scattering one takes at $y = 0$ $\Psi(0, u) = g_1 u$. As in the previous section the amplitude then generalizes the fan diagram case to include loops. We performed numerical evolution using (70) from $c_n(y = 0) = \delta_{n1}$ with a cutoff $n \leq N$. Again we took $\mu = 0.1$ and $\lambda = 0.01$. It turned out that a reliable solution could be found only at rapidities $y < 20$ when it practically does not depend on the cutoff. At higher rapidities one observes strong dependence of the cutoff, so that the solution could not be considered as reliable. This is illustrated in Fig. 10 in which the probabilities found by our procedure are shown at $y \leq 20$ and $y \geq 20$ in the left and right panels respectively. As a result the entropy corresponding to the calculated probabilities is uniquely found for $y < 20$ but has widely different values for different N at higher rapidities as shown in Fig. 11 together with the quasi-classical entropy (fans). As one observes the influence of quantum corrections is quite small at $y < 20$ but grows in an uncontrollable way at greater rapidities.

In conclusion, our recipe allows to construct probabilities $P_n(y)$ to find n pomerons at a given y as long as y is not so high, $y < 20$. At higher y coefficients $c_n(y)$ in the wave function cannot be found in a reliable manner. Then the solution of their evolution system (17) heavily depends on the chosen cutoff N . Actually at large n and y the coefficients $c_n(y)$ oscillate with ever growing amplitudes reaching very high orders of magnitude and so going beyond any reasonable precision in calculations.

AA scattering

For AA scattering the initial state is given by (10). So, in contrast to pA scattering, already at $y = 0$ the system is a superposition of states with different numbers of pomerons. In this case, putting $g_1 = 1$ $c_n(0) = -(-1)^n/n!$.

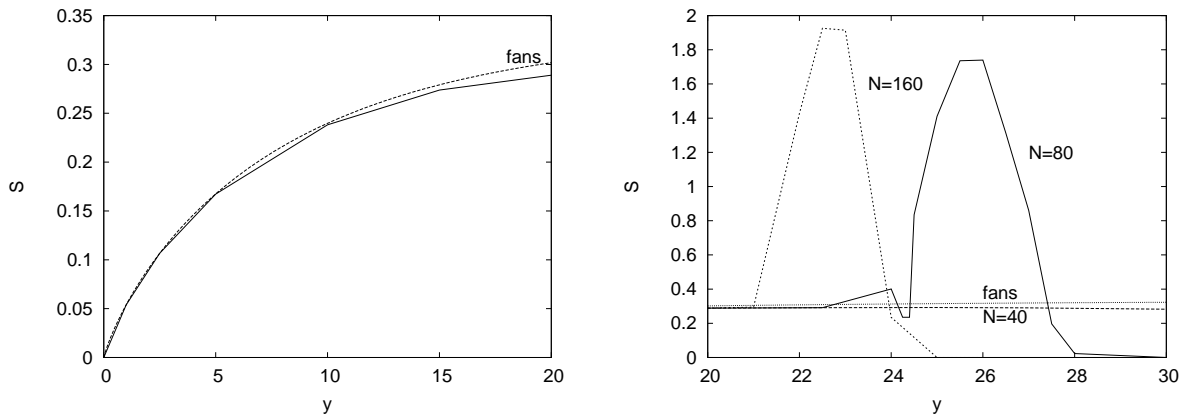


Figure 11: Entropy for pA scattering from the rescaling method with cutoff $n < N$ in the evolution equation for P_n for $y = 20$, independent of N , (left panel) and $y > 20$ for $N = 40, 80$ and 160 (right panel) Curves denoted as 'fans' show the quasi-classical entropy (36)

Acting according to our rescaling procedure we take the probabilities at $y = 0$ $P_n(0) = R^{-n}(0)/n!$ and from the normalization condition find $R(0) = 1/\ln 2$. So at $y = 0$ the probabilities are

$$P_n(0) = \frac{(\ln 2)^n}{n!}. \quad (72)$$

They strongly decrease as n grows. The corresponding entropy at $y = 0$ is naturally greater than zero. One finds

$$S(0) = 0.812166. \quad (73)$$

With the growth of rapidity the probabilities and entropy are to be found from the system of evolution equations (70) with the initial conditions $c_n(0)$. As before they depend on the cutoff $n < N$ in this system. Our results for the entropy are shown in Fig. 5 separately for $y < 15$ and $y > 15$. Similarly to the hA case reliable results, not depending on N , can only be obtained at $y < 18$, when the entropy grows monotonously from its value 0.812 at $y = 0$ to around unity at $y = 18$. At higher rapidities our results strongly depend on the cutoff and actually reflect a poorly controllable behavior of coefficients $c_n(y)$, which oscillate with ever greater amplitudes. To see it one can look upon the behavior of the scaling factor $R(y)$. At $y < 18$ it stays in the interval $1 < R < 8$ independent of N . But at greater y it abruptly blows up reaching values 10^7 at $y = 26$ for $N = 40$ and 10^6 already at $y = 22$ for $N = 80$. Such values lie outside the precision admitted in our evolution program.

7 Conclusions

We have studied the standard Regge-Gribov model with triple pomeron interactions from the point of view of the probabilistic interpretation, which has long been the subject of discussion. We draw attention to the fact that introduction of probabilities within this model is not unique and depends on what is meant under the relevant substructures, We have considered three different choices of these probabilities, namely the traditional partonic one, related to the reaction-diffusion approach and based on the partonic substructure of the pomeron, a pomeronic one based on the representation of the wave function in terms of multipomeron components and an alternative pomeronic one based on the number of pomeron propagators in the relevant Feynman diagrams. The three sorts of probabilities are very different and, which is more

important, behave very differently with the growth of energy. Their entropy either grows roughly linearly with rapidity or saturates and tends to a finite constant at large rapidities or, finally, first grows but then achieves a maximum and afterwards diminishes to zero as rapidity grows. Possible observable manifestation of these probabilities and entropy are also very different. While partonic quantities are supposedly to be seen in the spectra of emitted hadrons, the pomeronic ones are rather to be seen in the distributions of the cross-section in powers n assuming that their dependence of the coupling constants g to the participants is presented as a series in g^n . The partonic distributions in the probabilistic approach of [2, 1, 3, 12] seem to be external to TRGM and are imported into it from the QCD. They actually refer to the zero order in perturbation series in TRGM, that is to the single pomeron exchange. As a result conclusions in [12] about reaching an entangled state and scrambling at high energies do not seem to be directly related to our model but rather to the QCD interpretation of the pomeron in it.

Acknowledgment

The author is thankful for M.Lublinsky for numerous and helpful discussions.

References

- [1] S.Bondarenko, S.Motyka, A.H. Mueller, A.I.Shoshi and B.-W. Xiao, Eur. Phys. J. **C 50** (2007) 593
- [2] A. H. Mueller and G. P. Salam, Nucl. Phys. B 475, 293 (1996), G. P. Salam, Nucl. Phys. B 461, 512 (1996). [hep-ph/9509353].
- [3] M.A,Braun and G-P. Vacca, Eur. Phys. J. **C 50** (2007) 857.
- [4] J.-P. Blaizot, E. Iancu and D. N. Triantafyllopoulos, Nucl. Phys. A 784 (2007) 227. [hep-ph/0606253].
- [5] A. Kovner and M. Lublinsky, Nucl. Phys. A 767 171 (2006). [hep-ph/0510047].
- [6] A. Kovner, E. Levin and M. Lublinsky, JHEP 08 (2016), 031. [arXiv:1605.03251 [hep-ph]].
- [7] A. Kovner, E. Levin and M. Lublinsky, JHEP 05, 019 (2022) [arXiv:2201.01551 [hep-ph]].
- [8] A. Kovner, E. Levin and M. Lublinsky, [arXiv:2406.12691 [hep-ph]]
- [9] R.Jengo, Nucl. Phys. **B 108** (1976) 447.
- [10] D.Amati. I.Caneshi and R.Jengo, Nucl. Phys, **B 101** (1975) 397.
- [11] A.Schwimmer, Nucl. Phys. **B 437** (1995) 107
- [12] Kharzeev and E.Levin, Phys. Rev. **D 95** (2017) 114008.
- [13] M. Hentschinski and K. Kutak, Eur. Phys. J. C 82, 111 (2022), arXiv:2110.06156 [hep-ph].
- [14] M. Hentschinski, K. Kutak, and R. Straka, Eur. Phys. J. C 82, 1147 (2022), arXiv:2207.09430 [hep-ph].
- [15] V. A. Abramovsky, V. N. Gribov and O. V. Kancheli, Yad. Fiz. 18, 595-616 (1973), Sov. J. Nucl. Phys. 18, 308-317 (1974).